

# Plant-Derived Tandem Drug/Mesoporous Silicon Microcarrier Structures for Anti-Inflammatory Therapy

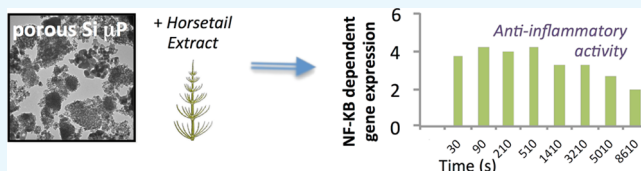
Jhansi R. Kalluri,<sup>†</sup> Julianna West,<sup>‡</sup> Giridhar R. Akkaraju,<sup>‡</sup> Leigh T. Canham,<sup>§</sup> and Jeffery L. Coffey<sup>\*,§,¶</sup>

<sup>†</sup>Department of Chemistry and Biochemistry and <sup>‡</sup>Department of Biology, Texas Christian University, Fort Worth, Texas 76129, United States

<sup>§</sup>Nanoscale Physics, Chemistry, and Engineering Research Laboratory, University of Birmingham, Birmingham B15 2TT, U.K.

## Supporting Information

**ABSTRACT:** The properties of nanostructured plant-derived porous silicon (pSi) microparticles as potential candidates to increase the bioavailability of plant extracts possessing anti-inflammatory activity are described in this work. pSi drug carriers were fabricated using an eco-friendly route from the silicon accumulator plant bamboo (tabasheer) powder by magnesiothermic reduction of plant-derived silica and loaded with ethanolic extracts of *Equisetum arvense*, another silicon accumulator plant rich in polyphenolic compounds. The anti-inflammatory properties of the active therapeutics present in this extract were measured by sensitive luciferase reporter assays; this active extract was subsequently loaded and released from the pSi matrix, with a clear inhibition of the activity of the inflammatory signaling protein NF- $\kappa$ B over a period of hours in a sustained manner. Our results showed that after loading the extracts of *E. arvense* into pSi microparticles derived from tabasheer, enhanced anti-inflammatory activity was observed owing to enhanced solubility of the extract.



## INTRODUCTION

Chronic inflammation is a condition implicated in several diseases including cancer,<sup>1</sup> Alzheimer's disease,<sup>2</sup> and rheumatoid arthritis.<sup>3</sup> Prolonged use of anti-inflammatory drugs is necessary in these cases to reduce associated inflammation. Nonsteroidal anti-inflammatory drugs (NSAIDs) and small biological molecules are a promising approach to treat this condition; however, long-term usage of NSAIDs are associated with serious side effects, thereby affecting the quality of life.<sup>4</sup> Other strategies involving the use of small biological drug molecules (e.g. chimeric monoclonal antibodies) have resulted in decreased therapeutic activity over time owing to drug resistance.<sup>5</sup>

One alternative for treating chronic inflammation is the use of plant extracts rich in polyphenolic compounds.<sup>6</sup> Some of the well-known polyphenols that have shown anti-inflammatory activity include curcumin,<sup>7</sup> epigallocatechin gallate,<sup>8</sup> and quercetin.<sup>9</sup> Synergistic anticancer activity of polyphenolic compounds has been observed in many cases; curcumin and catechin have shown high growth inhibition of human colon adenocarcinoma cells and use of quercetin and doxorubicin have demonstrated greater inhibition of cancer cells that are resistant to doxorubicin.<sup>10,11</sup> However, two of the major problems associated with the use of such compounds are their low bioavailability and relatively short half-life.<sup>8–13</sup> Because of this poor bioavailability, high oral doses or repeated dosing is often needed to reach an effective plasma concentration.

To address these challenges with polyphenolic-containing extracts, and to employ a nano/microscale drug carrier that is fabricated by a "green" route that avoids relatively toxic

reagents, we have encapsulated ethanolic extracts of *Equisetum arvense* (horsetail, itself a Si accumulator plant) into porous silicon (pSi) microparticles to increase their bioavailability. Such extracts were loaded into nanostructured pSi particles prepared by our previously optimized eco-friendly fabrication route from silicon accumulator plants.<sup>14–16</sup> Nanostructured pSi, typically prepared by anodization techniques, is an established drug delivery vehicle,<sup>17,18</sup> with broadly tunable porosities,<sup>19</sup> surface functionalities,<sup>20</sup> and resorptivity in vitro/in vivo.<sup>21–23</sup> Elemental pSi is utilized here rather than totally oxidized porous silica (SiO<sub>2</sub>) platforms such as diatoms,<sup>24,25</sup> as pSi provides a relatively more tunable resorptive profile as well as greater photostability of the active therapeutic within the pores.<sup>16</sup> In this study, the potential utility of pSi microparticles derived from tabasheer (*Concretio silicea bambusae*) loaded with ethanolic leaf extracts of *E. arvense* as a therapeutic agent was evaluated for anti-inflammatory properties. We have optimized entrapment techniques to efficiently load these *E. arvense* extracts into pSi particles in order to subsequently release anti-inflammatory components in a sustained fashion. Specifically, we have investigated the anti-inflammatory activity of ethanolic extracts of *E. arvense* released from pSi microparticles by studying their effect on the tumor necrosis factor  $\alpha$  (TNF $\alpha$ )-mediated nuclear factor  $\kappa$ -light-chain-enhancer of activated B cells (NF- $\kappa$ B) activation.

**Received:** January 14, 2019

**Accepted:** April 15, 2019

**Published:** May 9, 2019

NF- $\kappa$ B is a transcription factor regulating various cellular responses that are involved in a variety of cellular functions such as cell proliferation, apoptosis, as well as immune responses to infection and inflammation.<sup>26</sup> NF- $\kappa$ B molecules exist in most of the cells in an inactive form complexed with the inhibitory protein, I $\kappa$ B. In response to a stimulus (e.g. cytokines-IL-2 and TNF, viral infection, bacterial endotoxins, UV radiation) I $\kappa$ B kinase (IKK) enzyme phosphorylates I $\kappa$ B, leading to subsequent ubiquitination of I $\kappa$ B followed by proteasomal degradation. The removal of I $\kappa$ B reveals a nuclear localization sequence on NF- $\kappa$ B, which can now undergo nuclear translocation. NF- $\kappa$ B then attaches to specific binding sequences on the DNA and activates the transcription and secretion of a variety of proteins responsible for triggering inflammation.<sup>26</sup>

## RESULTS AND DISCUSSION

**Characterization of Plant-Derived pSi.** pSi particles were prepared by magnesiothermic reduction of silica extracted from tabasheer powder, according to a previously reported procedure.<sup>14–16</sup> Transmission electron microscopy (TEM) (Figure 1a) of a typical reaction product shows a highly porous

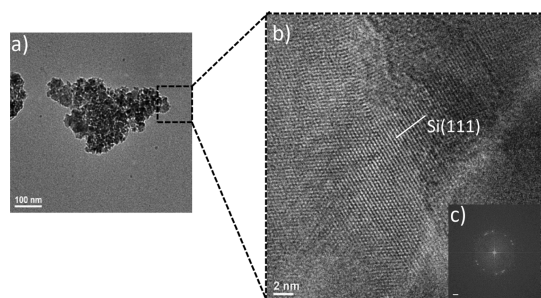


**Figure 1.** (a) Low-magnification TEM image of a freestanding pSi microparticle; (b) high-resolution TEM image shows the (111) planes of cubic Si; (c) FFT of the associated silicon nanocrystalline region (scale bar 2 nm).

nanoscale morphology for these particles; the average pSi particle size estimated by TEM analysis is  $1300 \pm 400$  nm (Figure S1); high-resolution TEM imaging (Figure 1b) shows a lattice spacing of 0.310 nm associated with the (111) index of cubic Si. The fast Fourier transform (FFT) associated with this

image (inset) is consistent with a polycrystalline orientation of the Si in this matrix.

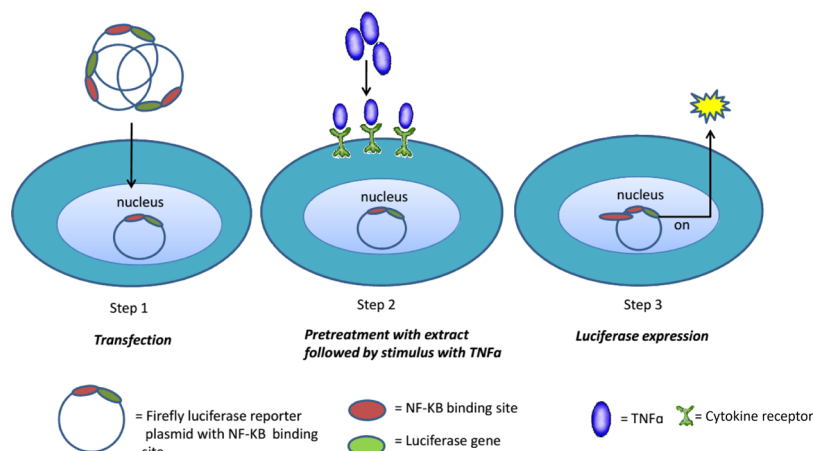
As noted in previous studies, pSi particles derived by such a route using this silicious-rich substance derived from the nodal joints of bamboo have a nanostructured morphology that is best described as mesoporous (dominant pore sizes in the range of 2–50 nm). This material is composed of Si nanostructures embedded in a rough oxide-rich matrix; surface areas on the order of  $150 \text{ m}^2$  per gram are typically obtained.

**Testing the Anti-Inflammatory Activity of *E. arvense* Extract.** Prior to loading into the porous Si drug carrier, the anti-inflammatory activity of an extract of *E. arvense* (harvested from a natural source in Malvern, Worcestershire, UK) was examined by monitoring its ability to inhibit TNF $\alpha$ -mediated activation of the NF- $\kappa$ B gene promoter with a luciferase assay. Scheme 1 illustrates a schematic representation of the luciferase assay.

HEK 293 cells were treated with an ethanolic extract of *E. arvense* for 1 h followed by stimulation with 10 ng/mL of TNF $\alpha$ . As a positive control for inhibition, cells were transfected with I $\kappa$ B $\Delta$ N, a dominant negative inhibitor of NF- $\kappa$ B, which has the phosphorylation sites mutated, rendering it unable to be ubiquitinated and degraded. Cells treated with extracts at concentrations of 200  $\mu\text{g}/\text{mL}$  (w/v) showed significant decreases in luciferase production (concomitant with an inhibition of NF- $\kappa$ B-mediated gene expression), demonstrating that the extract inhibited the TNF $\alpha$ -induced activation of NF- $\kappa$ B. The ability of this extract to inhibit NF- $\kappa$ B gene expression was compared to a commercially available anti-inflammatory drug, diclofenac sodium; in our experiments, at similar concentrations, the extract shows a comparable level of inhibition relative to diclofenac sodium (Figure 2).

**Characterization of *E. arvense* Extract-Loaded pSi.** pSi microparticles were subsequently impregnated with an *E. arvense* ethanol leaf extract by a solution loading method. A mixture of solvents, ethanol, water, and dimethyl sulfoxide (DMSO), were used in the ratio of 2:2:1 by volume. DMSO was used as a co-solvent to enhance the concentration of extract in the solution. Loading capacity was evaluated by thermogravimetric analysis (TGA) and physical state of the extract after loading into pSi was evaluated by powder X-ray diffraction (XRD) and differential scanning calorimetry (DSC).

**Scheme 1. Schematic Representation of the Luciferase Assay**



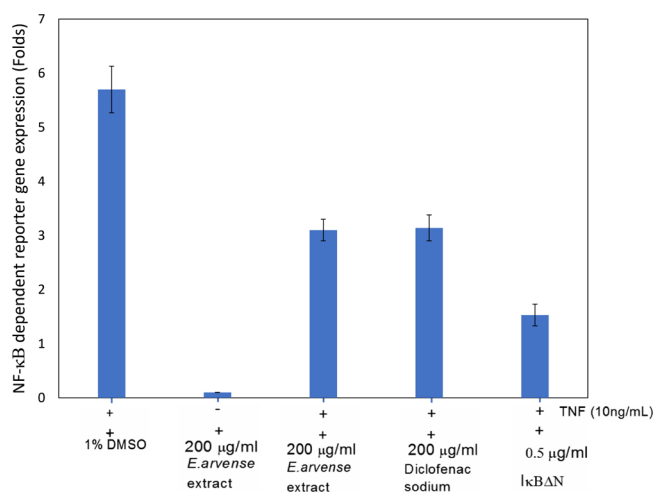


**Figure 2.** Inhibition of NF-κB-dependent reporter gene expression by *E. arvensis* extract, diclofenac (known anti-inflammatory drug), and IκBΔN (positive control). Cells were treated with 10 ng/mL of TNFα to induce NF-κB gene activation. The presence and absence of TNF and extract are denoted by symbols (+) and (-), respectively.

**Thermogravimetric Analysis.** The extract was loaded into pSi with a theoretical loading of ~30% by weight. TGA was used to analyze the loading capacity of the extract into pSi microparticles. Mass loss profile was observed between 25 and 350 °C, which may include evaporation of the solvent mixture along with partial removal of the crude extract components (Figure S2). The observed mass loss,  $15.0 \pm 2.0\%$ , is assumed (within this temperature range) to underestimate the amount of loaded extract owing to incomplete removal of all the components of the extract.

**Differential Scanning Calorimetry.** Major phenolic constituents of the *E. arvensis* extract are kaempferol and quercetin.<sup>27</sup> An overlay of DSC thermograms is shown in the Supporting Information Figure S3 for an *E. arvensis* extract and extract-loaded pSi. The DSC trace of the *E. arvensis* extract shows two endothermic events in the range of 50–150 and 200–350 °C. Melting within 50–150 °C can be attributed to evaporation of water, co-solvent, or residual extract components with low melting points. The second melting peak in the DSC trace within the range of 200–350 °C is likely a consequence of the melting of major phenolic constituents kaempferol and quercetin, with melting points of 276 and 316 °C, respectively. Such values fall within the melting range (200–350 °C) of this extract. From these observations, one can infer that these two compounds are indeed present in the *E. arvensis* ethanol extract. After loading the extract into pSi, the DSC trace shows a clear shift in the melting peak to a lower range, consistent with a reduction in crystallite size of the components in the extract as a consequence of pore confinement.<sup>28,29</sup>

**XRD Analysis.** Figure 3 shows an overlay of XRD diffractograms obtained for pSi microparticles, an *E. arvensis* dried extract, and an *E. arvensis* extract loaded into pSi derived from tabasheer. The diffraction pattern of the *E. arvensis* extract alone with the most intense peaks at 26°, 41°, 51°, and 67° indicates the presence of highly crystalline phases in such a mixture. Assuming that the above loaded concentration of extract in the pSi particles is within the detection limit of the XRD, the absence of these peaks after loading into pSi microparticles suggests that some nanostructuring of the

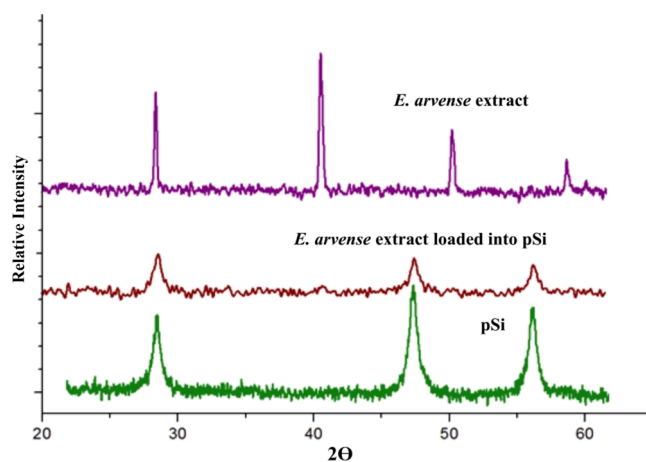


**Figure 3.** XRD analysis of *E. arvensis* dry extract, before and after loading into pSi microparticles.

extract components takes place upon its loading into the porous Si matrix.<sup>30</sup>

**In Vitro Release of Anti-Inflammatory Extract.** As pointed out above, *E. arvensis* is rich in polyphenolic compounds, having poor solubility in aqueous buffered media.<sup>31</sup> Similar observations were qualitatively noted here while loading an *E. arvensis* extract into pSi particles. When the *E. arvensis* extract was initially dispersed in water, the addition of organic solvents (ethanol and DMSO) greatly enhanced the solubility of the extract. In vitro release of the anti-inflammatory extract was monitored by a luciferase assay. Figure 4 shows the release profile of bulk soluble extract and

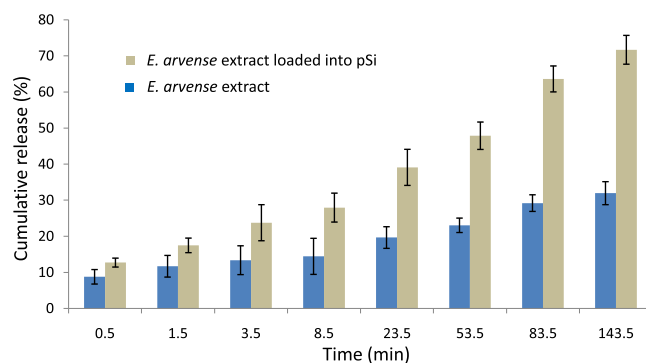


**Figure 4.** In vitro release of the anti-inflammatory components from pSi loaded with *E. arvensis* extract. Statistical differences between the two categories beyond 0.5 min are confirmed by ANOVA analyses ( $P < 0.05$ ).

extract loaded into pSi. After a short duration (3.5 min), at any given time point the amount of the soluble extract released from pSi is significantly higher than the bulk extract itself. There is no notable difference (<5%) between the amount of soluble extract released from pSi and just the extract itself at time points of 0.5 and 1.5 min. This is confirmed by a statistical analysis of these two categories over the timescale of the release experiment [analysis of variance (ANOVA)]; only for the initial time point of 0.5 min are the two categories indistinguishable ( $P = 0.1$ ); for the remaining release points, the categories are clearly statistically different [ $P$  values ranging from 0.03 (1.5 min) to 0.001 (143.5 min)]. This similarity within the first 2 min of release can be attributed to surface

bound crystalline extract present outside the pSi microparticles that has similar solubility profiles as that of the bulk crystalline extract. Any surface-bound fraction present on pSi particles is either due to pore overfilling or a recrystallized portion of the extract that is present within the pores of Si microparticles. A marked difference (>10%) in the amount of soluble extract released from pSi and the extract was observed at later points of time from 3.5 to 143.5 min. This suggests that the gradual release of the pore-confined extract components in nanostructured form (as noted from the above DSC and XRD measurements) enhanced the solubility of the extract. At the end of 143.5 min, the cumulative release of the soluble extract from pSi is twofold higher than the extract alone.

**Anti-Inflammatory Activity of the Released *E. arvense* Extract.** We also quantified the anti-inflammatory activity of the released extract to explore the possible difference between the activity of the extract and extract loaded into pSi. As described in the [Experimental Section](#), the amount of extract released at a given time point was added to the HEK 293 cells, and the luciferase gene expression was measured using a luminometer. The limitation of the assay is that only 100  $\mu\text{L}$  of the extract released into the sterile water at a given time point is able to be added to the cells to minimize the dilution of growth medium (needed for healthy cell growth). The minimum dose required (*E. arvense*) to show anti-inflammatory activity by this assay is 40  $\mu\text{g}/\text{mL}$ . This means that every 100  $\mu\text{L}$  of the extract should contain at least 400  $\mu\text{g}$  of the extract to show any observable anti-inflammatory activity. Owing to the limitations of the assay protocol all the test samples collected at each time point are spiked with a known concentration of the extract to clearly visualize the enhanced anti-inflammatory activity of the extract after loading into pSi. [Figure 5](#) shows the levels of luciferase activity in the presence

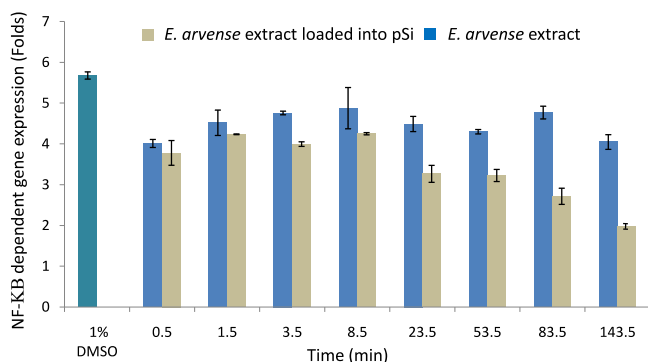


**Figure 5.** Anti-inflammatory activity of the *E. arvense* extract and extract-loaded pSi powders. All samples were spiked with (50  $\mu\text{g}/\text{mL}$ ) of *E. arvense* extract. Statistical differences between the two categories beyond 8.5 min are confirmed by ANOVA analyses ( $P < 0.05$ ).

of extract released from pSi and bulk extract alone. We used 1% DMSO-treated HEK 293 cells as our control. Anti-inflammatory compounds should ideally decrease the luciferase expression by blocking NF- $\kappa\text{B}$  activation. We observed reduced luciferase gene expression compared to the control (1% DMSO), thereby showing the anti-inflammatory nature of the *E. arvense* extract. Beyond the 8.5 min release point, enhanced anti-inflammatory activity was observed in the case of extract loaded into pSi compared to just the extract itself. For the data shown in [Figure 5](#), the expression levels are statistically comparable from the 0.5 to 8.5 min window ( $P \approx$

0.1), but are different at 23.5 min release and beyond ( $P < 0.001$ ). A notable difference (0.5 fold) in the anti-inflammatory activity was observed at the 143.5 min release point, owing to the likely enhanced solubility of the extract after loading into pSi.

Overall, in these experiments we have demonstrated that pSi microparticles derived from tabasheer can serve as effective controlled release carriers to entrap and release anti-inflammatory polyphenolic components with otherwise poor aqueous solubility. Combined results from XRD and DSC measurements showed that *E. arvense* actives can be entrapped into pSi in a more soluble form (presumably owing to nanostructuring of the extract components). This is a strikingly similar phenomenon to that observed previously in the case of pSi loaded with hydrophobic antibacterial compounds such as triclosan.<sup>32–34</sup> These similarities indicate that mesoporous morphologies of plant-derived pSi microparticles are capable of loading either a single active component or a complex multicomponent mixture (as in this case) in a more soluble form, thereby ideally enhancing its bioavailability. Expanding the number of possible examples utilizing this ability of porous Si to improve this parameter continues.

## EXPERIMENTAL SECTION

**Instrumentation.** TGA was performed using a Seiko SII model SSC/5200 TGA at a heating rate of 10  $^{\circ}\text{C}/\text{min}$  (up to 400  $^{\circ}\text{C}$ ) under nitrogen. DSC analysis was done using a DSC 2 system (Mettler Toledo). Duplicate measurements were made using TGA and DSC. A given sample was placed into a Al pan with a hole on top and heated from 25 to 400  $^{\circ}\text{C}$  at the rate of 10  $^{\circ}\text{C}/\text{min}$ , under nitrogen flush. XRD was carried out using a Phillips 3100 X-ray powder diffractometer with Cu  $K\alpha$  radiation operating at 35 kV. Luciferase gene expression was measured by a Berthold SIRIUS II luminometer. Field emission SEM and energy dispersive X-ray analysis was conducted with a JEOL JSM-7100F operating at 15 kV. TEM imaging was performed using a JEOL JEM-2100.

**Soxhlet Extraction of *E. arvense* Leaves.** *E. arvense* leaves and stems were harvested from a natural source in Malvern, Worcestershire, UK in fall 2016. The obtained leaves were shade-dried for two days. Ground powder (6 g) was extracted with 50% ethanol (100 mL) at a temperature of 120  $^{\circ}\text{C}$  in a Soxhlet extractor. After 6 h, the extract was concentrated through the use of rotary evaporator, and the dry extracts were stored at 4  $^{\circ}\text{C}$  for further analysis.

**Loading of *E. arvense* Leaf Extract into pSi.** Leaf extract was loaded into tabasheer-derived pSi particles using a solution loading method. Dried extract powder (3.4 mg) was dissolved in a solvent mixture of ethanol, water, and DMSO (2:2:1 by volume). Extract solution (150  $\mu\text{L}$ ) was added to the pSi particles (10.2 mg). The mixture was then dried under vacuum overnight.

**Cell Lines and Culture.** The HEK 293 (human embryonic kidney fibroblast) cell line was used for all experiments. The cells were maintained in Dulbecco's modified Eagle's medium supplemented with 10% heat-inactivated fetal bovine serum, penicillin–streptomycin (88 U/mL penicillin and 88  $\mu\text{g}/\text{mL}$  streptomycin), L-glutamine (0.88 mM), and 1/100 minimum essential medium non-essential amino acids (Sigma #M7145). The cells were grown at 37  $^{\circ}\text{C}$  in an atmosphere of 5%  $\text{CO}_2$  and 95% air.

**Luciferase Assay.** A luciferase activity assay was used to measure the luciferase gene expression triggered by TNF $\alpha$ -

induced activation of NF- $\kappa$ B. HEK 293 cells were treated with the anti-inflammatory extract released from the pSi particles. All the samples were run in triplicate. HEK 293 cells were plated in 24-well plates with a cell density of 50 000/well. After 24 h, cells were transfected (step 1) with two plasmids RLCMV-LUC (5 ng/mL *Renilla* sp.); PRDII-LUC (10 ng/mL firefly) using a commercial transfecting agent LyoVec (Invitrogen). PRDII-LUC plasmid has an NF- $\kappa$ B binding site and luciferase reporter (LUC) gene. RLCMV-LUC (5 ng/mL; *Renilla* sp.) with a constitutively active human cytomegalovirus immediate early promoter driving luciferase reporter gene is used as an internal control, so that by normalizing the activity, the experimental variability (e.g. cell viability or transfection efficiency) will be minimized. After 48 h of transfection, the cells were treated with different concentrations of anti-inflammatory extract (100  $\mu$ L) prepared in 1% DMSO (step 2); 1 h later the cells were stimulated with 10 ng/mL of TNF $\alpha$  and 5 h later, the cells were harvested and lysed with passive lysis buffer (100  $\mu$ L/well, Promega, Dual-Luciferase assay kit). The luciferase assays were performed according to the manufacturer's assay protocol, and luminescence produced by luciferase gene expression was measured by a luminometer (step 3).

**Standard Curve for the *E. arvense* Extract (Anti-Inflammatory Activity).** A stock solution was prepared by dissolving 9 mg of *E. arvense* extract in 1 mL of 2% DMSO. Standard solutions of the extract were added to the wells to give final concentrations of extract per well ranging from 40 to 300  $\mu$ g/mL. The final concentration of DMSO in each well is 1%. The luminescence observed from the expression of luciferase is recorded by a luminometer. Supporting Information Figure S4 shows the standard curve with a concentration of the extract plotted against the luciferase expression.

**In Vitro Release of *E. arvense* Extract from pSi Microparticles.** In vitro release of the *E. arvense* extract from the pSi particles was monitored by a luciferase assay for the release of anti-inflammatory compounds. All the samples were run in triplicates. pSi microparticles loaded with the *E. arvense* extract (5 mg) as well as samples of solid *E. arvense* extract itself (1.5 mg) were placed in two different vials with 1 mL of sterilized water and agitated at 30 rpm. At the end of a given time point, the vials were centrifuged for 2 min at 500 rpm, the supernatant was removed and replenished with 1 mL of fresh sterilized water. The supernatant containing the soluble extract (100  $\mu$ L) was added to the 24-well plate seeded with a cell density of 5000 cells/well. The amount of anti-inflammatory compounds released from pSi and the extract itself at a chosen time period is below the detection limit of the luciferase assay. A standard addition method was used to bring the concentration levels within the range of the standard curve. All the wells are treated with a known concentration of the extract (50  $\mu$ g/mL). The actual amount of soluble extract released at a given time point was quantified in reference to a standard curve developed by the luciferase assay.

## ■ ASSOCIATED CONTENT

### ● Supporting Information

The Supporting Information is available free of charge on the ACS Publications website at DOI: 10.1021/acsomega.9b00127.

TEM images/histogram of pSi particles; standard curve for the luciferase anti-inflammatory activity for *E. arvense* extract; and TGA and DSC data of *E. arvense* extract-loaded pSi (PDF)

## ■ AUTHOR INFORMATION

### Corresponding Author

\*E-mail: j.coffer@tcu.edu.

### ORCID

Jeffery L. Coffey: 0000-0003-0267-9646

### Author Contributions

J.R.K., G.R.A., L.T.C., and J.L.C. conceived and planned the experiments; J.R.K. prepared and characterized all pSi samples, as well as their loading with anti-inflammatory extracts and subsequent release bioassays; J.W. and J.R.K. carried out the luciferase assays on the *E. arvense* extracts; J.L.C., G.R.A., and L.T.C. provided overall supervision for the project; J.R.K., G.R.A., J.L.C., and L.T.C. analyzed the data and wrote the paper.

### Funding

Financial support by the Robert A. Welch Foundation (grant P-1212) is gratefully acknowledged.

### Notes

The authors declare no competing financial interest.

## ■ ACKNOWLEDGMENTS

The authors gratefully thank Professor Csilla Gergely of the University of Montpellier for useful discussions.

## ■ REFERENCES

- (1) Balkwill, F.; Coussens, L. M. Cancer: an inflammatory link. *Nature* **2004**, *431*, 405–406.
- (2) Rosenblum, W. I. Why Alzheimer trials fail: removing soluble oligomeric beta amyloid is essential, inconsistent, and difficult. *Neurobiol. Aging* **2014**, *35*, 969–974.
- (3) Freund, A.; Orjalo, A. V.; Desprez, P.-Y.; Campisi, J. Inflammatory networks during cellular senescence: causes and consequences. *Trends Mol. Med.* **2010**, *16*, 238–246.
- (4) Bost, J. W.; Maroon, J. C.; Maroon, A. Natural anti-inflammatory agents for pain relief. *Surg. Neurol. Int.* **2010**, *1*, 80.
- (5) Emami-Shahri, N.; Hagemann, T. Resistance—the true face of biological defiance. *Rheumatology* **2012**, *51*, 413–422.
- (6) Karunaweera, N.; Raju, R.; Gyengesi, E.; Münch, G. Plant polyphenols as inhibitors of NF- $\kappa$ B induced cytokine production—a potential anti-inflammatory treatment for Alzheimer's disease? *Front. Mol. Neurosci.* **2015**, *8*, 24.
- (7) Jobin, C.; Bradham, C. A.; Russo, M. P.; Juma, B.; Narula, A. S.; Brenner, D. A.; Sartor, R. B. Curcumin blocks cytokine-mediated NF- $\kappa$ B activation and proinflammatory gene expression by inhibiting inhibitory factor I- $\kappa$ B kinase activity. *J. Immunol.* **1999**, *163*, 3474–3483.
- (8) Kim, J.; Lee, H. J.; Lee, K. W. Naturally occurring phytochemicals for the prevention of Alzheimer's disease. *J. Neurochem.* **2010**, *112*, 1415–1430.
- (9) Endale, M.; Park, S.-C.; Kim, S.; Kim, S.-H.; Yang, Y.; Cho, J. Y.; Rhee, M. H. Quercetin disrupts tyrosine-phosphorylated phosphatidylinositol 3-kinase and myeloid differentiation factor-88 association, and inhibits MAPK/AP-1 and IKK/NF- $\kappa$ B-induced inflammatory mediators production in RAW 264.7 cells. *Immunobiology* **2013**, *218*, 1452–1467.
- (10) Shehzad, A.; Lee, J.; Huh, T.-L.; Lee, Y. S. Curcumin induces apoptosis in human colorectal carcinoma (HCT-15) cells by regulating expression of Prp4 and p53. *Mol. Cell* **2013**, *35*, 526–532.

- (11) Lv, L.; Liu, C.; Chen, C.; Yu, X.; Chen, G.; Shi, Y.; Li, G. Quercetin and doxorubicin co-encapsulated biotin receptor-targeting nanoparticles for minimizing drug resistance in breast cancer. *Oncotarget* **2016**, *7*, 32184–32199.
- (12) Anand, P.; Kunnumakkara, A. B.; Newman, R. A.; Aggarwal, B. B. Bioavailability of curcumin: problems and promises. *Mol. Pharm.* **2007**, *4*, 807–818.
- (13) Shen, L.; Liu, C. C.; Ann, C. Y.; Ji, H. F. How does curcumin work with poor bioavailability? Clues from experimental and theoretical studies. *Sci. Rep.* **2016**, *6*, 20872.
- (14) Batchelor, L.; Loni, A.; Canham, L. T.; Hasan, M.; Coffey, J. L. Manufacture of mesoporous silicon from living plants and agricultural waste: an environmentally friendly and scalable process. *Silicon* **2012**, *4*, 259–266.
- (15) Kalluri, J. R.; Gonzalez-Rodriguez, R.; Hartman, P. S.; Loni, A.; Canham, L. T.; Coffey, J. L. Single plant derived nanotechnology for synergistic antibacterial therapies. *PLoS One* **2016**, *11*, No. e0163270.
- (16) Le, N. T.; Kalluri, J. R.; Loni, A.; Canham, L. T.; Coffey, J. L. Biogenic nanostructured porous silicon as a carrier for stabilization and delivery of natural therapeutic species. *Mol. Pharm.* **2017**, *14*, 4509–4514.
- (17) Anglin, E.; Cheng, L.; Freeman, W.; Sailor, M. Porous silicon in drug delivery devices and materials. *Adv. Drug Delivery Rev.* **2008**, *60*, 1266–1277.
- (18) Salonen, J.; Kaukonen, A. M.; Hirvonen, J.; Lehto, V.-P. Mesoporous silicon in drug delivery applications. *J. Pharm. Sci.* **2008**, *97*, 632–653.
- (19) Loni, A. In *Handbook of Porous Silicon*, 1st ed.; Canham, L., Ed.; Springer International Publishing: New York, 2014; pp 11–22.
- (20) Buriak, J. M. Organometallic chemistry on silicon and germanium surfaces. *Chem. Rev.* **2002**, *102*, 1271–1308.
- (21) Anderson, S. H. C.; Elliott, H.; Wallis, D. J.; Canham, L. T.; Powell, J. J. Dissolution of different forms of partially porous silicon wafers under simulated physiological conditions. *Phys. Status Solidi A* **2003**, *197*, 331–335.
- (22) Godin, B.; Gu, J.; Serda, R. E.; Bhavane, R.; Tasciotti, E.; Chiappini, C.; Liu, X.; Tanaka, T.; Decuzzi, P.; Ferrari, M. Tailoring the degradation kinetics of mesoporous silicon structures through PEGylation. *J. Biomed. Mater. Res., Part A* **2010**, *94*, 1236–1243.
- (23) Tzur-Balter, A.; Shatsberg, Z.; Beckerman, M.; Segal, E.; Artzi, N. Mechanism of erosion of nanostructured porous silicon drug carriers in neoplastic tissues. *Nat. Commun.* **2015**, *6*, 6208.
- (24) Yoo, J.-W.; Irvine, D. J.; Discher, D. E.; Mitragotri, S. Bio-inspired, bioengineered and biomimetic drug delivery carriers. *Nat. Rev. Drug Discovery* **2011**, *10*, 521.
- (25) Goes, A.; Fuhrmann, G. Biogenic and biomimetic carriers as versatile transporters to treat infections. *ACS Infect. Dis.* **2018**, *4*, 881–892.
- (26) Taniguchi, K.; Karin, M. NF- $\kappa$ B, inflammation, immunity and cancer: coming of age. *Nat. Rev. Immunol.* **2018**, *18*, 309–324.
- (27) Gründemann, C.; Lengen, K.; Sauer, B.; Garcia-Käufer, M.; Zehl, M.; Huber, R. *Equisetum arvense* (common horsetail) modulates the function of inflammatory Immunocompetent cells. *BMC Complementary Altern. Med.* **2014**, *14*, 283.
- (28) Riikonen, J.; Mäkilä, E.; Salonen, J.; Lehto, V.-P. Determination of the Physical State of Drug Molecules in Mesoporous Silicon with Different Surface Chemistries. *Langmuir* **2009**, *25*, 6137–6142.
- (29) Lehto, V.-P.; Vähä-Heikkilä, K.; Paski, J.; Salonen, J. Use of thermoanalytical methods in quantification of drug load in mesoporous silicon microparticles. *J. Therm. Anal. Calorim.* **2005**, *80*, 393–397.
- (30) Mäkilä, E.; Ferreira, M. P. A.; Kivelä, H.; Niemi, S.-M.; Correia, A.; Shahbazi, M.-A.; Kauppila, J.; Hirvonen, J.; Santos, H. A.; Salonen, J. Confinement Effects on Drugs in Thermally Hydrocarbonized Porous Silicon. *Langmuir* **2014**, *30*, 2196–2205.
- (31) Kaur, H.; Kaur, G. A Critical Appraisal of Solubility Enhancement Techniques of Polyphenols. *J. Pharm.* **2014**, *2014*, 180845.
- (32) Wang, M.; Coffey, J. L.; Dorraj, K.; Hartman, P. S.; Loni, A.; Canham, L. T. Sustained antibacterial activity from triclosan-loaded nanostructured mesoporous silicon. *Mol. Pharm.* **2010**, *7*, 2232–2239.
- (33) Tang, L.; Saharay, A.; Fleischer, W.; Hartman, P. S.; Loni, A.; Canham, L. T.; Coffey, J. L. Sustained Antifungal Activity from a Ketoconazole-Loaded Nanostructured Mesoporous Silicon Platform. *Silicon* **2013**, *5*, 213–217.
- (34) Wang, M.; Hartman, P. S.; Loni, A.; Canham, L. T.; Bodiford, N.; Coffey, J. L. Influence of Surface Chemistry on the Release of an Antibacterial Drug from Nanostructured Porous Silicon. *Langmuir* **2015**, *31*, 6179–6185.